dmj
DIABETES & METABOLISM JOURNAL

Semaglutide and Exercise Synergy in Obesity: Preserving Muscle Mass and Uncovering Organ Crosstalk

José A. Inia, Simone Droog, Jessica Snabel, Aswin L. Menke, Martien P.M. Caspers, Jelle C.B.C. de Jong, J. Wouter Jukema, Hans M.G. Princen, Anita M. van den Hoek

Diabetes Metab J Published online Jul 15, 2026 | *https://doi.org/10.4093/dmj.2025.1060*

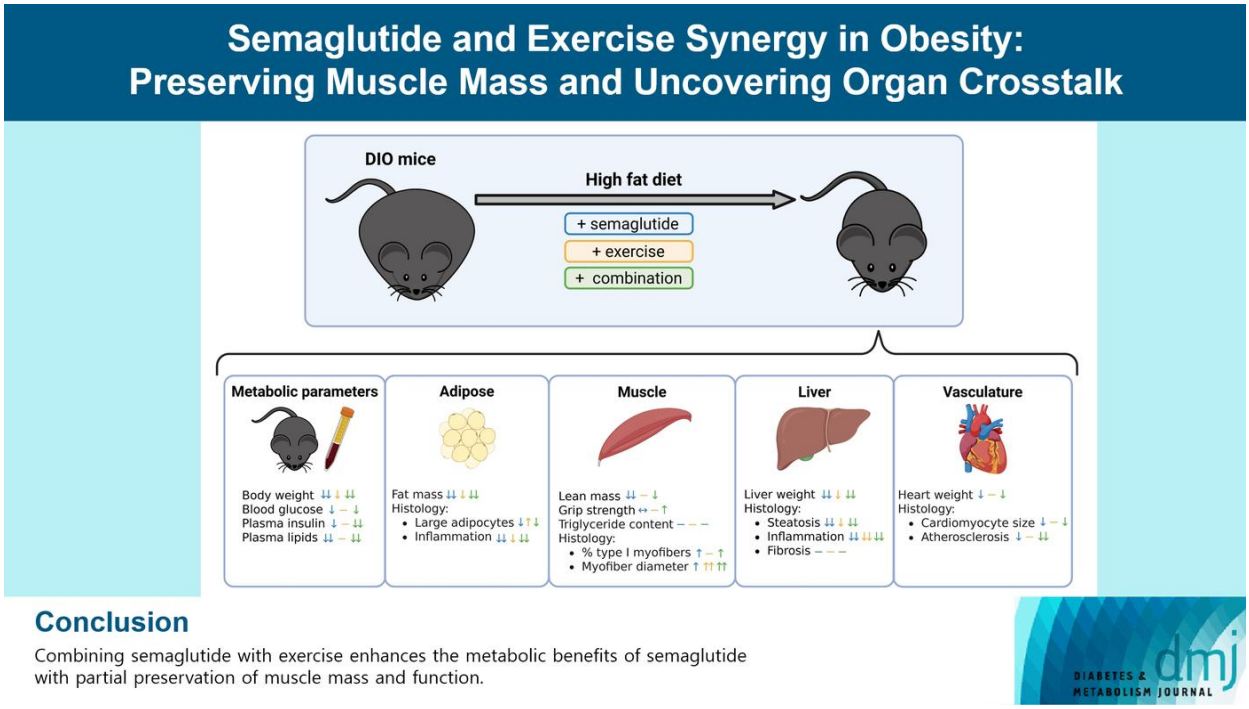

Highlights

- **Semaglutide induces weight loss but reduces lean mass and muscle strength as well.**
- **Exercise attenuates semaglutide-induced loss of lean mass.**
- **Combining semaglutide with exercise enhances muscle strength and myofiber diameter.**
- **Multi-organ transcriptomics reveal synergistic, organ-specific pathway activation.**

How to cite this article:
Inia JA, Droog S, Snabel J, Menke AL, Caspers MPM, Jong JCBC, et al. Semaglutide and Exercise Synergy in Obesity: Preserving Muscle Mass and Uncovering Organ Crosstalk. Diabetes Metab J Published online Jul 15, 2026. https://doi.org/10.4093/dmj.2025.1060

Original Article
Basic and Translational Research

Diabetes Metab J Published online Jul 15, 2026
https://doi.org/10.4093/dmj.2025.1060
pISSN 2233-6079 · eISSN 2233-6087

dmj
DIABETES & METABOLISM JOURNAL

Semaglutide and Exercise Synergy in Obesity: Preserving Muscle Mass and Uncovering Organ Crosstalk

José A. Inia[1,2,3], Simone Droog[1], Jessica Snabel[1], Aswin L. Menke[1], Martien P.M. Caspers[4], Jelle C.B.C. de Jong[4], J. Wouter Jukema[2,3,5], Hans M.G. Princen[1], Anita M. van den Hoek[1]

[1]Department of Metabolic Health Research, The Netherlands Organization for Applied Scientific Research (TNO), Leiden, the Netherlands
[2]Department of Cardiology, Leiden University Medical Center, Leiden, the Netherlands
[3]Einthoven Laboratory for Experimental Vascular Medicine, Leiden University Medical Center, Leiden, the Netherlands
[4]Department of Microbiology and Systems Biology, The Netherlands Organization for Applied Scientific Research (TNO), Leiden, the Netherlands
[5]Netherlands Heart Institute, Utrecht, the Netherlands

Background: Semaglutide, a glucagon-like peptide-1 receptor agonist, effectively promotes weight loss and improves metabolic parameters in individuals with obesity. However, its use is often accompanied by reductions in lean mass, raising concerns about long-term muscle health. This study explored whether combining semaglutide with exercise could preserve muscle mass and enhance metabolic outcomes.
Methods: Ldlr−/−.Leiden mice with diet-induced obesity, insulin resistance, metabolic dysfunction-associated steatohepatitis and atherosclerosis were either left untreated (control) or treated with semaglutide, exercise or the combination for 14 weeks. Histological and transcriptomic analyses were conducted on adipose tissue, muscle, liver and heart to explore underlying mechanisms.
Results: Semaglutide significantly reduced fat mass (−31%) but also lean mass (−11%). Combining semaglutide with exercise further reduced fat mass (−45%) and lean mass as well but to a lesser extent (−8%). Semaglutide alone or with exercise improved insulin sensitivity and plasma lipids. The combination improved adipose tissue inflammation, liver steatosis, liver inflammation and atherosclerotic lesion area. Only combination treatment significantly improved grip strength and diameter of gastrocnemius myofibers. Multi-organ histological and transcriptomic analyses revealed organ-specific and synergistic effects of combination therapy, including activation of pathways involved in mitochondrial function, glucose metabolism, and inflammation resolution.
Conclusion: Semaglutide improves metabolic, liver, vascular and adipose parameters but reduces lean mass and muscle strength. Combining semaglutide intervention with exercise enhances these benefits with partial preservation of muscle mass and function and activation of distinct molecular pathways not engaged by either monotreatment, thereby underscoring the potential of integrating lifestyle interventions with pharmacological treatment.

Keywords: Exercise; Gene expression profiling; Glucagon-like peptide 1; Life style; Muscular atrophy; Sarcopenia; Semaglutide

INTRODUCTION

In recent years, glucagon-like peptide-1 (GLP-1) receptor agonists, including semaglutide, have gained widespread attention for their efficacy in managing obesity. Although initially developed for glycemic control in patients with type 2 diabetes mellitus, they were revealed to have substantial weight-lowering effects as well [1,2]. This dual action resulted in their approval as the first pharmacological intervention specifically indicated for treatment of obesity [3]. Their mechanisms of action, ranging from delayed gastric emptying and enhanced insulin secretion to appetite suppression and altered lipid metabolism, are now well characterized [4,5].

Nevertheless, concerns have been raised regarding the rapid

Corresponding author: José A. Inia https://orcid.org/0000-0002-3725-6785
Department of Metabolic Health Research, The Netherlands Organization for Applied Scientific Research (TNO), Sylviusweg 71, 2333 BE Leiden, the Netherlands
E-mail: jose.inia@tno.nl

Received: Oct. 22, 2025; Accepted: Mar. 29, 2026

weight loss induced by semaglutide, as the reductions in body weight involve a concurrent reduction in lean body mass as well. Skeletal muscle is not only essential for mobility and strength but also plays a crucial role in maintaining insulin sensitivity and metabolic homeostasis. While the pleiotropic effects of semaglutide are well documented, the long-term metabolic effects, particularly those related to loss of lean mass, remain poorly understood. Preservation of lean body mass during semaglutide-induced weight loss is therefore essential to mitigate the risk of sarcopenia.

We hypothesized that combining semaglutide intervention with exercise could preserve muscle mass, thereby optimizing body composition as well as metabolic and functional outcomes. To investigate this, we used diet-induced obese Ldlr−/−.Leiden mice, a mouse model that recapitulates key features of the metabolic syndrome when fed a high-fat diet (HFD), including insulin resistance, hyperlipidemia, metabolic dysfunction-associated steatohepatitis (MASH) and atherosclerosis [6-11]. These animals were treated with semaglutide, exercise or the combination thereof, and changes in body composition were followed in time. Multi-tissue histological and transcriptomic analyses were conducted to elucidate the molecular mechanisms and inter-organ communication underlying the physiological responses to semaglutide and exercise, and to explore their potential synergistic effects.

METHODS

Detailed information on experimental methods can be found in the Supplementary Methods.

Experimental design

Experimental procedures were approved by the governmental central committee on animal experiments (AVD5010020172064) and an independent Animal Welfare body of The Netherlands Organization for Applied Scientific Research (IVD TNO; TNO-558). Animals were bred and housed at an AAALAC-accredited specific pathogen-free animal facility (TNO Metabolic Health Research, Leiden, the Netherlands). The Ldlr−/−.Leiden mouse model was chosen because these mice develop characteristics of the metabolic syndrome including obesity, insulin resistance, hyperlipidemia, metabolic dysfunction-associated steatotic liver disease (MASLD) with fibrosis and atherosclerosis when fed an HFD.

Statistical analysis

All data are presented as mean±standard error of the mean (SEM). Non-parametric testing was done to determine differences between groups. To this end, Kruskal-Wallis testing was performed, followed by Mann-Whitney *U* testing for independent samples. All statistical analyses were performed using SPSS software version 29.0.2.0 (IBM Co., Armonk, NY, USA). Two-tailed *P* values are reported and a $P<0.05$ was considered statistically significant.

For transcriptome analysis, differentially expressed pathways (DEPs) and upstream regulators (URs) were selected based on pathway enrichment (*P* value Fisher's exact test <0.01) and z-score for directionality. A z-score <−2 indicates a predicted reduced activity and a z-score >2 indicates a predicted increased activity based on the direction of gene expression changes of target genes.

RESULTS

Semaglutide alone and with exercise improves metabolic parameters in obese Ldlr−/−.Leiden mice

HFD feeding increased body weight (21% vs. chow) (Fig. 1A) without any significant difference in food intake (Fig. 1B). The increase in body weight was primarily due to an increase in fat mass (67%), with lean mass unchanged (Fig. 1C and D). HFD decreased insulin sensitivity, as reflected by a 2-fold increase in plasma insulin levels ($P=0.065$, vs. chow) (Fig. 1E). Plasma cholesterol, triglycerides and alanine transaminase (ALT) were increased as well, while blood glucose remained similar in HFD-fed versus chow-fed mice (Supplementary Fig. 1A-D).

Semaglutide intervention during the last 14 weeks precluded the increase in body weight (−19%) (Fig. 1A), driven by decreases in fat (−31%) and lean mass (−11%) (Fig. 1C) versus HFD control. Exercise alone reduced body weight by 6%, mainly through fat mass reduction (−13%) while maintaining lean mass. Combining semaglutide with exercise profoundly reduced body weight (−24% vs. HFD control), with fat and lean mass reduced by 45% and 8%, respectively. Although lean mass was lower at the study endpoint, it appeared higher throughout the study in the combination group versus semaglutide alone (Fig. 1D). All semaglutide-treated mice showed a temporary decline in calorie intake during the first week, which normalized thereafter (Fig. 1B). Semaglutide alone and with exercise improved glucose (semaglutide: −15%; combination: −17%) (Supplementary Fig. 1A) and insulin levels (semaglutide:

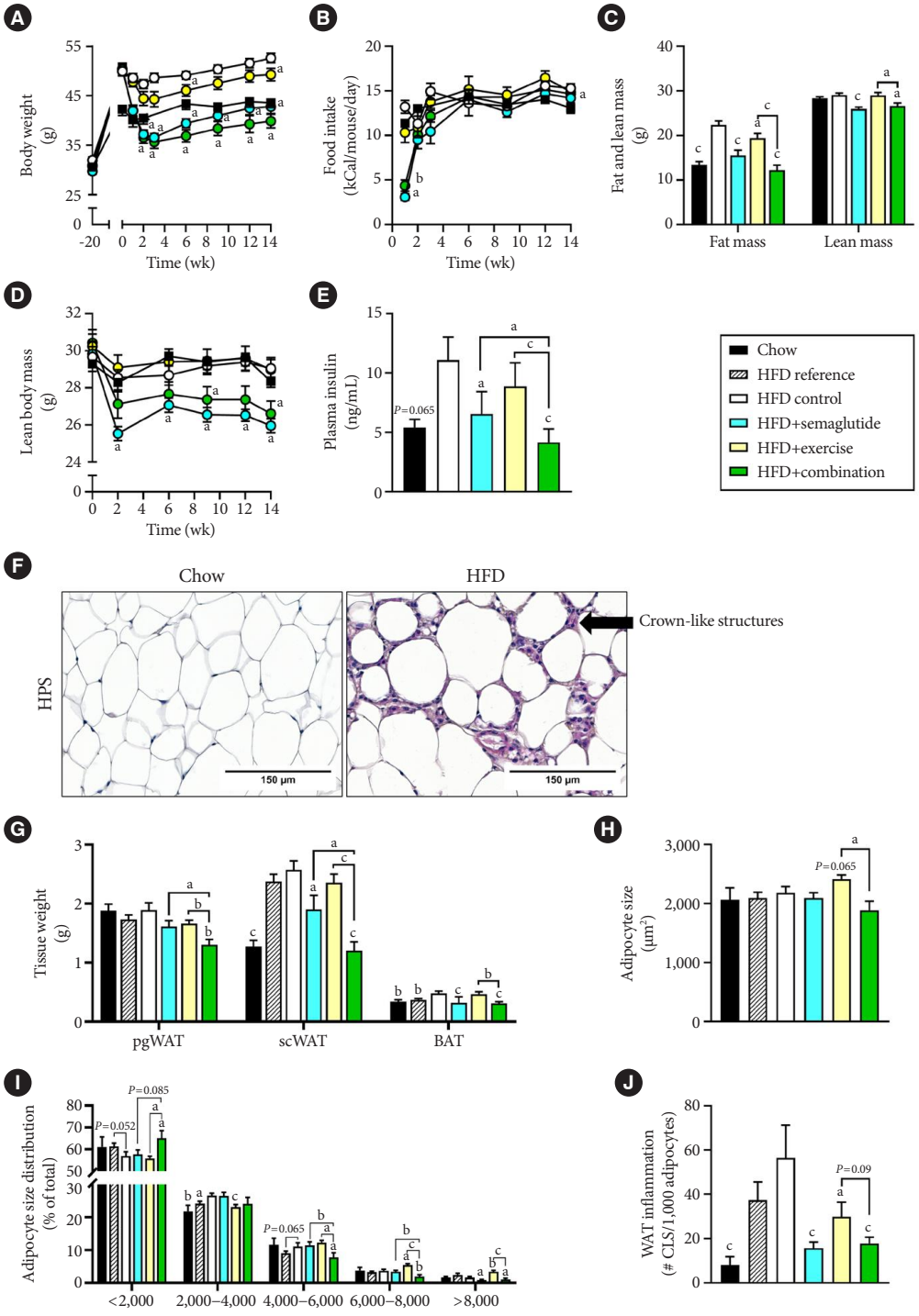

Fig. 1. Semaglutide alone and with exercise improve metabolic parameters in obese Ldlr−/−.Leiden mice and reduce white adipose tissue (WAT) inflammation. Body weight (A), food intake (B), fat and lean mass (endpoint) (C), lean mass over time (D) and plasma insulin (E). Representative images of WAT cross-sections stained with hematoxylin-phloxine-saffron (HPS; arrow indicates Crown-like structures) (F). Weights of perigonadal WAT (pgWAT), subcutaneous WAT (scWAT) and brown adipose tissue (BAT) (G), adipocyte size (H), adipocyte size as percentage of total adipocytes (I) and WAT inflammation (J). Values are presented as mean±standard error of the mean for $n=14$–15 mice. CLS, Crown-like structure. [a]$P<0.05$, [b]$P<0.01$, [c]$P<0.001$ vs. high-fat diet (HFD) control.

–41%; combination: –62%) (Fig. 1E) relative to untreated controls, with insulin significantly lower in the combination group than semaglutide monotreatment group (–36%), indicating enhanced insulin sensitivity. Cholesterol and triglyceride levels were reduced by semaglutide alone (both –33%), tended to be reduced by exercise (cholesterol: –13%, $P=0.089$; triglycerides: –24%, $P=0.098$) and were significantly reduced by the combination (–35% and –47%, respectively) (Supplementary Fig. 1B and C). Plasma ALT concentrations were reduced by semaglutide (–71%), exercise (–28%), and the combination (–77%) relative to untreated controls (Supplementary Fig. 1D). Similarly, semaglutide and the combination of semaglutide and exercise reduced plasma levels of the fibrosis surrogate marker TIMP metallopeptidase inhibitor 1 (TIMP1) (Supplementary Fig. 1E).

Semaglutide, exercise, and the combination reduce white adipose tissue inflammation

Thirty-four weeks of HFD feeding increased subcutaneous white adipose tissue (scWAT; 100%) and brown adipose tissue (BAT; 43%) mass, while perigonadal white adipose tissue (pgWAT) remained unchanged (Fig. 1G). Relative to HFD controls, semaglutide reduced scWAT (–26%) and BAT (–33%) weight, while pgWAT remained similar. Exercise alone did not affect adipose depot weights. Conversely, combination treatment had the strongest effect, significantly reducing pgWAT (–31%), scWAT (–53%) and BAT (–36%) weights versus HFD controls and pgWAT (–25%) and scWAT (–49%) versus HFD reference. Compared to semaglutide alone, the combination further lowered pgWAT (–20%) and scWAT (–37%).

Histological analysis of pgWAT (Fig. 1F) revealed no increase in adipocyte size in HFD controls versus aging chow-fed mice (Fig. 1H). Surprisingly, exercise tended to increase adipocyte size (11%, $P=0.065$), but not when combined with semaglutide. More detailed analysis revealed that semaglutide reduced the percentage of large hypertrophic adipocytes (>8,000 μm^2) (–47%) (Fig. 1I). Exercise increased adipocytes in the 6,000 to 8,000 μm^2 (69%) and >8,000 μm^2 (44%) ranges. Conversely, combination treatment increased the percentage of small adipocytes (<2,000 μm^2) (7%) and reduced medium and large ones (4,000–6,000: –33%; 6,000–8,000: –48%; >8,000: –34%). Since larger adipocytes promote inflammation [12], crown-like inflammatory structures were quantified (Fig. 1F and J). Inflammation was significantly reduced by semaglutide (–72%), exercise (–47%), and the combination (–68%), with both semaglutide-treated groups reaching levels below start of treatment HFD reference.

Combination of semaglutide and exercise improves muscle function

Since exercise partly prevented semaglutide-induced lean mass loss (Fig. 1D), muscle parameters were further analyzed. HFD feeding reduced relative weight of gastrocnemius and soleus (–9% vs. chow) (Fig. 2B). Only the combination treatment with semaglutide and exercise increased their weight versus HFD controls (20%) and versus semaglutide (13%). Grip strength was impaired in HFD controls (–32% vs. chow) and was significantly improved by the combination treatment only (17%) (Fig. 2C).

In the soleus, HFD feeding reduced the percentage of slow (type I) myofibers versus chow-fed mice (–15%) (Fig. 2A and D). Semaglutide alone or with exercise, restored slow myofibers levels to those observed in chow-fed mice (15% and 18%, respectively, vs. HFD control), while exercise alone had no effect.

In the gastrocnemius, HFD feeding reduced myofiber size (minimal Feret's diameter) (–10% vs. chow) (Fig. 2E). Semaglutide tended to increase myofiber size (4%, $P=0.0502$), while exercise (8%) and the combination (9%) significantly increased this. Despite reduced absolute muscle weight, combination intervention increased myofiber diameter, a discrepancy that was not due to changes in intramuscular triglyceride content, which remained stable across groups (Fig. 2F).

Mechanistic effects were further studied by assessing the effects of semaglutide on myotube differentiation and function in C2C12 cells (Fig. 2G). In differentiating C2C12 cells, prostaglandin D_2 (negative control) reduced myofiber size (–39% vs. phosphate-buffered saline) while semaglutide had no effect (Fig. 2H), indicating the *in vivo* increase in myofiber size is not due to direct action on muscle cells. Semaglutide also did not affect myotube differentiation (fusion index, Supplementary Fig. 2A) or glucose uptake, while insulin (positive control) did increase glucose uptake (11%) (Fig. 2I). Furthermore, plasma concentrations of the inflammatory myokine interleukin 6 were not significantly affected by semaglutide, exercise, or the combination (Supplementary Fig. 2B). Similarly, semaglutide and exercise alone did not affect plasma levels of the marker of neuro-muscular signaling brain-derived neurotrophic factor (BDNF), while combination treatment significantly increased plasma BDNF levels (Supplementary Fig. 2C). Finally, plasma

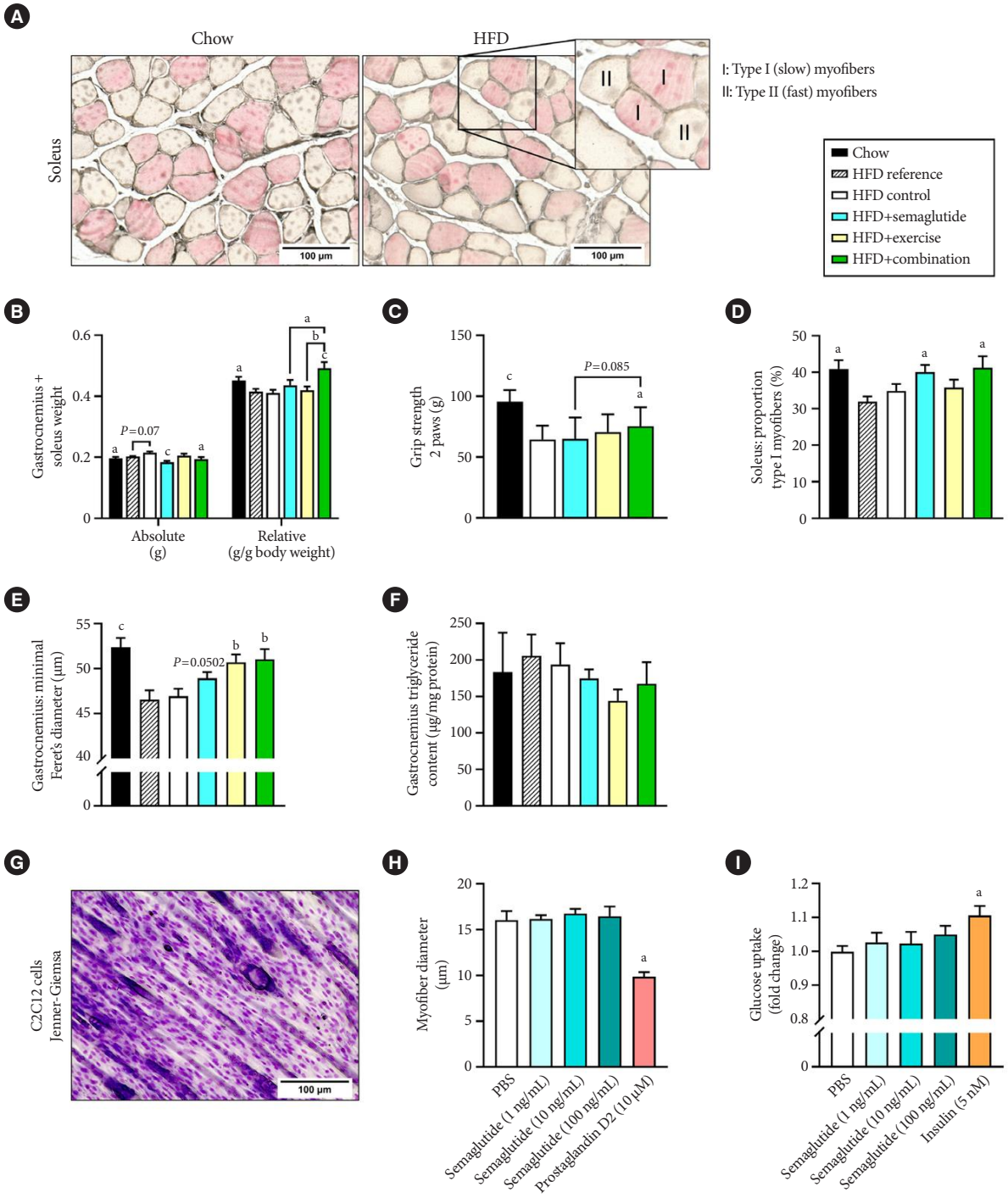

Fig. 2. Combination of semaglutide with exercise improves muscle function. Representative images of soleus muscle cross-sections stained with anti-myosin heavy chain 7 (MYH7) (slow, type I fibers) and laminin (basal lamina) (A). Weight of the gastrocnemius and soleus muscle, absolute values and relative to body weight (B), 2-paw grip strength (C), percentage of type I myofibers in the soleus muscle (D), minimal Feret's diameter of myocytes in the gastrocnemius muscle (E), triglyceride content of the gastrocnemius muscle (F). *In vitro* experiment in C2C12 myotubes with representative image of a Jenner-Giemsa staining (G), myofiber diameter (H) and glucose uptake (I). Values are presented as mean ± standard error of the mean for $n=14–15$ mice (B-F) or for $n=3–6$ measurements per condition *in vitro* (H-I). $^{a}P<0.05$, $^{b}P<0.01$, $^{c}P<0.001$ vs. high-fat diet (HFD) control (B-F) or phosphate-buffered saline (PBS) (H-I).

levels of the muscle-specific marker myostatin significantly reduced with HFD feeding relative to chow controls, but increased with semaglutide, exercise, or combination intervention (Supplementary Fig. 2D). These findings suggest that semaglutide-induced changes in muscle morphology are likely mediated through indirect mechanisms.

Semaglutide alone and with exercise has beneficial effects on hepatic steatosis and inflammation but not fibrosis

Thirty-four weeks on HFD increased liver weight (43% vs. chow), which was partially reversed by semaglutide (–39%), exercise (–19%), and their combination (–46%) (Fig. 3B). Histological analysis (Fig. 3A) revealed that semaglutide reduced macrovesicular (–65%) and microvesicular (–43%) steatosis, exercise reduced macrovesicular steatosis (–43%) and the combination had additive effects on macrovesicular steatosis (–79% vs. HFD control; –41% vs. semaglutide; –64% vs. exercise) (Fig. 3C and D). Additionally, microvesicular steatosis was almost completely abolished in the combination treatment group (–98% vs. HFD control).

Hepatic inflammation, minimal in chow-fed mice, was markedly elevated in HFD-fed mice, with aggregates of mononuclear and polymorphonuclear cells visible at intervention start (HFD reference; Fig. 3E). Hepatic inflammation was significantly reduced by semaglutide (–81%), exercise (–66%), and their combination (–89%) versus HFD controls, even below levels observed in the HFD reference group.

HFD feeding induced hepatic fibrosis (Fig. 3A and F), which progressed during the intervention period (Fig. 3F). However, fibrosis was not significantly affected by semaglutide, exercise or the combination relative to HFD control group (Fig. 3F). Similarly, fibrosis stage was not affected by either intervention, with fibrosis present within perisinusoidal and periportal areas (stage F2) and bridging fibrosis (stage F3) (Fig. 3G).

Combining semaglutide intervention with exercise reduces cardiac mass, cardiomyocyte size and atherosclerotic lesion area

HFD feeding induced an increase in heart weight (15% vs. chow), which was reversed by semaglutide alone (–13%) and in combination with exercise (–11%), but not by exercise alone (Fig. 4B). Similarly, semaglutide reduced cardiomyocyte size (semaglutide: –11%; combination: –15% vs. HFD control) (Fig. 4C).

Ldlr–/–.Leiden mice naturally develop atherosclerosis during aging, which can be aggravated by HFD feeding (Fig. 4A). HFD feeding for 34 weeks increased total cholesterol exposure (concentration×weeks) throughout the whole study (2.5-fold increase vs. chow) (Fig. 4D). Despite lower cholesterol levels during the final 14 weeks, none of the interventions reduced total cholesterol exposure.

Elevated cholesterol exposure induces atherosclerosis development (Fig. 4A), illustrated by a 3.3-fold increase in atherosclerotic lesion area in HFD-fed mice (vs. chow) (Fig. 4E). Semaglutide tended to reduce lesion area (–20%, $P=0.067$) and while exercise did not affect lesion area, combination treatment significantly reduced lesion area (–27%). Lesion severity, already high in chow-fed mice, worsened with HFD (Fig. 4F) but was not significantly affected by any intervention. However, combination intervention resulted in 35% fewer severe lesions compared to semaglutide alone.

Differential effects of semaglutide, exercise and combination intervention on transcriptomics profile

Histological analysis of white adipose tissue (WAT), muscle, liver and hearts, revealed substantial benefits of semaglutide, exercise and their combination. Next generation sequencing identified DEPs across treatments and tissues (Fig. 5, Venn diagrams proportional in size). Semaglutide predominantly affected gene expression in the liver, while exercise mainly impacted muscle tissue. Overlap between interventions was minimal in WAT, modest in aorta, and more pronounced in muscle and liver. Combination of semaglutide with exercise induced many new pathways, especially in WAT and aorta, while losing other pathways, demonstrating that combination treatment was not merely the sum of monotreatments. The combination treatment clearly affected the most pathways, with the most pronounced effects observed in the liver.

In WAT, semaglutide affected a modest number of DEPs ($n=88$), albeit more than exercise monotreatment ($n=48$). The top 15 most enriched pathways (Fig. 5A) demonstrate that semaglutide influenced diverse signaling pathways, while exercise mainly upregulated inflammatory and metabolic pathways. For combination intervention, 58% of pathways enriched by semaglutide monotreatment overlapped, while this overlap with exercise monotreatment was only 15%. Notably, the combination treatment activated 211 novel pathways not observed in either monotreatment. These were primarily related to signaling and cancer-associated processes, with most genes showing reduced expression, underscoring a distinct synergistic effect.

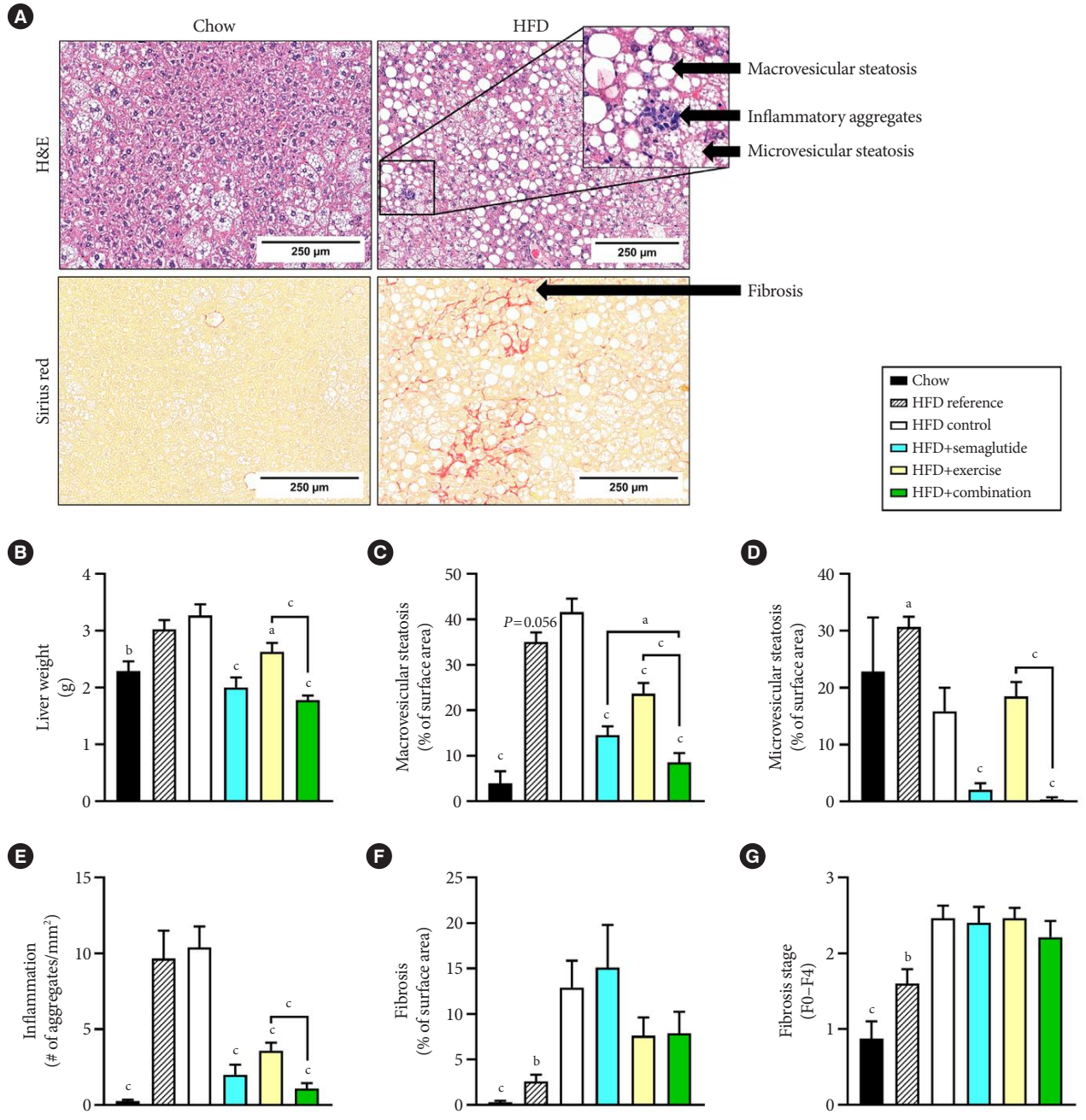

Fig. 3. Semaglutide with exercise reduces hepatic steatosis and inflammation but not fibrosis. Representative histological images of liver cross-sections stained with hematoxylin and eosin (H&E; arrows indicate areas with macrovesicular and microvesicular steatosis and aggregated inflammatory cells) and Sirius Red (arrow indicates area with fibrosis) (A). Liver weight (B), macrovesicular steatosis (C) and microvesicular steatosis (D) as percentage of surface area, inflammation as number of inflammatory aggregates (E), fibrosis as percentage of surface area (F) and fibrosis stage (F0–F4) (G). Values are presented as mean ± standard error of the mean for $n = 14$–15 mice. $^{a}P<0.05$, $^{b}P<0.01$, $^{c}P<0.001$ vs. high-fat diet (HFD) control.

In the gastrocnemius, semaglutide affected 131 pathways, with the top 15 most enriched pathways mainly involved in metabolic and inflammatory processes (Fig. 5B). Exercise had strong effects on muscle (152 DEPs), for the top 15 DEPs especially involved in mitochondrial processes and with most genes upregulated. Combination of semaglutide with exercise in-

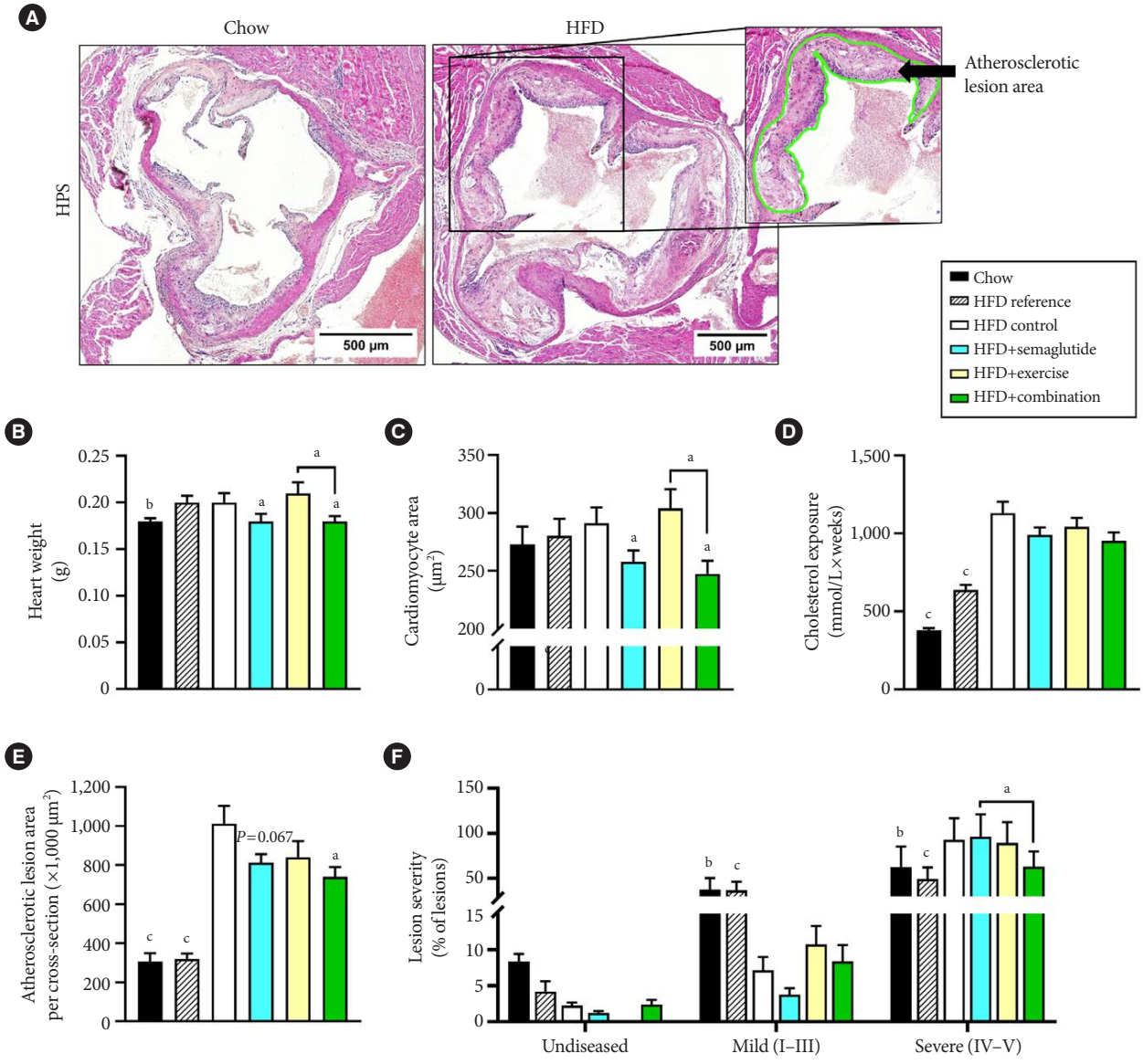

Fig. 4. Combining semaglutide with exercise reduces heart weight, cardiomyocyte size and atherosclerotic lesion area. Representative images of hematoxylin-phloxine-saffron (HPS)-stained cross-sections of the aortic root area (lesion area of interest indicated in green) (A). Heart weight (B), cardiomyocyte area (C), total cholesterol exposure (D), atherosclerotic lesion area (E) and lesion severity (F). Values are presented as mean±standard error of the mean for $n=14$–15 mice. $^{a}P<0.05$, $^{b}P<0.01$, $^{c}P<0.001$ vs. high-fat diet (HFD) control.

duced differential expression of $n=143$ pathways that largely (75%) overlapped with both monotreatments and introducing 36 new pathways. The top 15 of those additional pathways were largely involved in metabolic processes, including glucose metabolism and insulin signaling, which were not affected by either monotreatment in muscle.

In liver, the effect of semaglutide was largest ($n=457$ DEPs), with the top 15 most enriched pathways involved in metabolic, inflammatory and signaling processes (Fig. 5C). Exercise alone had minimal effects in the liver ($n=31$), mostly affecting mitochondrial and metabolic pathways. Combination intervention altered $n=531$ pathways, largely overlapping with those induced by semaglutide alone, including all top 100 DEPs. Additionally, 143 unique pathways were induced in the combination intervention group, for the top 15 primarily related to fibrotic and mitochondrial processes.

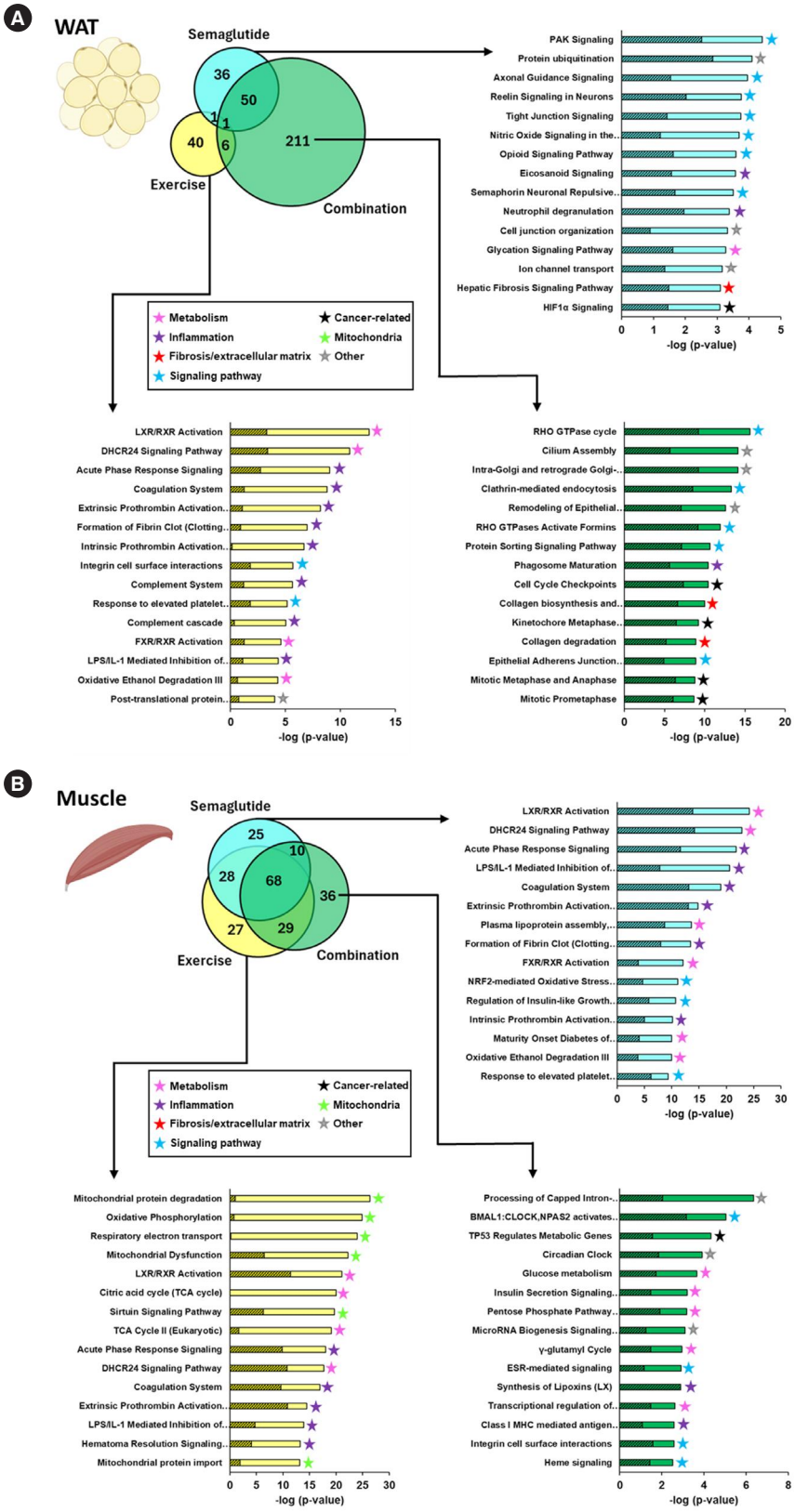

Fig. 5. Continued to the next page.

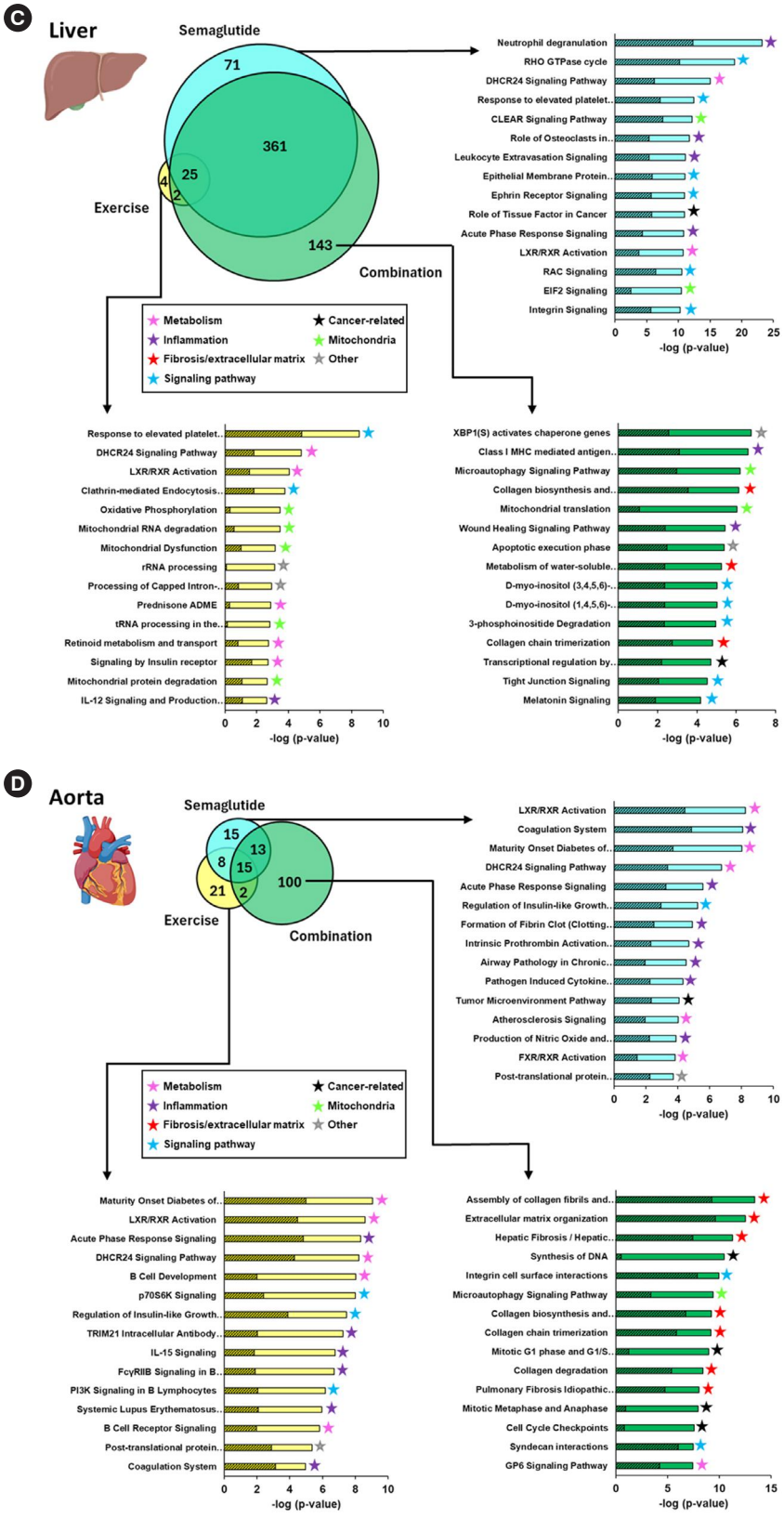

Fig. 5. Continued to the next page.

Fig. 5. Venn diagrams illustrating the overlap of differentially expressed pathways. Differentially expressed pathways in white adipose tissue (WAT) (A), muscle (B), liver (C) and aorta (D) between Ldlr−/−.Leiden mice receiving semaglutide vs. untreated mice (blue circle), mice that received exercise intervention vs. untreated mice (yellow circle) or mice receiving the combination of semaglutide and exercise vs. untreated mice (green circle). The top 15 most significantly enriched are shown for different portions of the Venn diagram, i.e., the genes affected by semaglutide treatment (blue bars), the genes affected by exercise (yellow bars) and the genes uniquely affected by combination treatment (green bars). Hatched bars represent downregulated genes, open bars represent upregulated genes. PAK, p21-activated kinase; LXR, liver X receptor; RXR, retinoid X receptor; DHCR24, 24-dehydrocholesterol reductase; FXR, farnesoid X receptor; LPS, lipopolysaccharide; IL-1, interleukin 1; GTPase, guanoside triphosphatase; TCA, tricarboxylic acid; BMAL1, brain and muscle arnt-like 1; CLOCK, circadian locomotor output cycles kaput; NPAS2, neuronal PAS domain protein 2; MHC, major histocompatibility complex; CLEAR, coordinated lysosomal expression and regulation; RAC, Ras-related C3 botulinum toxin substrate; EIF2, eukaryotic initiation factor 2; ADME, absorption, distribution, metabolism, and excretion; XBP1, X box binding protein 1; TRIM21, tripartite motif containing 21; FcγRIIB, Fc gamma receptor IIb.

Among the four organs, the aorta showed the least DEPs. Semaglutide affected 51 pathways, primarily involved in metabolic and inflammatory processes (Fig. 5D), including atherosclerosis signaling, consistent with observed atherosclerotic lesion reductions (Fig. 4). Exercise enriched $n=46$ pathways involved in similar processes. Combination intervention induced $n=130$ pathways with limited overlap with both monotreatments ($n=30$) and $n=100$ unique pathways of which the top 15 were primarily involved in fibrosis and collagen synthesis.

Semaglutide and exercise have synergistic effects on key upstream regulators

In an UR analysis, the predicted activation or deactivation states (z-score) of URs, e.g., transcription factors, signaling proteins and metabolites, are determined based on downstream gene expression. Fig. 6 displays the top eight (or less if not available) most significantly upregulated (z-score >2.0) and top eight most significantly downregulated (z-score <−2.0) URs in WAT, muscle, liver and aorta for each intervention.

In WAT, semaglutide enhanced activation of URs across various processes, including reduced activity of glycogen synthase kinase-3 beta (GSK3B; glycogen metabolism) and acyl-CoA synthetase long chain family member 4 (ACSL4; fatty acid metabolism). Exercise strongly activated URs linked to glucose homeostasis, such as hepatocyte nuclear factor 4 alpha (HNF4A) and HNF1A. Combination of semaglutide with exercise strongly downregulated URs including immunoglobulin E, interferon alpha, transforming growth factor beta 1 (TGFB1), and colony stimulating factor 2 (CSF2), further substantiating the anti-inflammatory effects observed at the histological level.

In muscle, semaglutide activated URs involved in lipid and sterol metabolism (Niemann-Pick type C1 [NPC1], cytochrome P450 family 7 subfamily B member 1 [CYP7B1]) and deactivated URs involved in glucose homeostasis (HNF4A, HNF1A, adiponectin, C1Q and collagen domain containing [ADIPOQ]). Exercise activated URs central to energy metabolism, glucose homeostasis and mitochondrial health (PPARG coactivator 1 alpha [PPARGC1A], insulin receptor [INSR], frataxin [FXN]). The combination treatment activated shared URs from both monotreatments (CYP7B1, FXN, calcium binding protein 39 like [CAB39L]) and similarly deactivated URs involved in glucose and lipid metabolism (HNF4A, HNF1A, ADIPOQ, dual specificity tyrosine phosphorylation regulated kinase 1B [DYRK1B]).

In the liver, semaglutide activated URs involved in inflammation and lipid metabolism, consistent with histological improvements in steatosis and inflammation. Notably, immunity-related GTPase family M member 1 (Irgm1; a suppressor of inflammasome activation) and MLX interacting protein like (MLXIPL; central in glucose metabolism) were strongly activated, while inflammatory cytokines such as interferon alpha, CSF2, and interleukin 33 were deactivated. Exercise alone had minimal effects, with only four URs deactivated across various processes. The combination treatment largely mirrored the effects of semaglutide monotreatment, with slightly broader UR activation and deactivation.

In aorta tissue, semaglutide mainly deactivated URs linked to immune activation (CSF2, IL1A, tumor necrosis factor [TNF], interferon gamma [IFNG], mitogen-activated protein kinase kinase kinase 8 [MAP3K8]). Exercise predominantly deactivated URs involved in lipid and glucose metabolism (nuclear receptor subfamily 1 group H member 4 [NR1H4], PPARG, ADIPOQ, HNF1A, HNF4A). The combination treatment had the strongest effects, activating URs related to extracellular matrix remodeling and fibrosis (FKBP prolyl isomerase 10 [FKBP10], collagen type V alpha 1 chain [COL5A1],

	Semaglutide			Exercise			Combination		
	Upstream regulator	Activation z-score	-log 10 overlap p-value	Upstream regulator	Activation z-score	-log 10 overlap p-value	Upstream regulator	Activation z-score	-log 10 overlap p-value
WAT	ARID1A	3.1	4.2	HNF4A	4.5	12.7	mir-21 (includes of	5.9	7.7
	CAPN6	2.8	2.6	HNF1A	4.1	17.7	let-7a-5p (and othe	5.7	6.4
	USF2	2.4	2.6	NFkB (complex)	3.4	2.5	NUPR1	5.4	8.0
	miR-124-3p (and c	2.2	3.7	SMARCAL1	3.2	5.8	PNPLA2	5.4	4.5
	EHMT1	2.1	2.1	ADIPOQ	3.0	5.6	PEAR1	5.2	9.9
	VCAN	2.1	2.9	SMARCB1	2.8	2.7	alpha catenin	5.2	6.5
	FTO	2.1	3.3	PKD1	2.6	2.4	miR-30c-5p (and c	5.1	5.3
				NCOA2	2.6	7.0	CDKN1A	5.1	16.9
	PTEN	-2.0	2.8	CYP7B1	-2.2	4.4	BHLHE40	-6.1	2.4
	TWF1	-2.1	3.2	TRIM24	-2.2	2.2	IgE	-6.1	3.6
	PGR	-2.2	5.5	NR0B2	-2.4	6.1	TBX3	-6.3	14.4
	TFEB	-2.2	3.2	EGLN	-2.4	2.2	TFEB	-6.3	24.4
	CG	-2.3	2.1	SMARCA5	-2.4	2.7	interferon alpha	-6.5	3.2
	ACSL4	-2.4	2.3	TGFBR2	-2.5	2.4	TGFB1	-6.7	21.5
	KRAS	-2.6	6.0	HFE	-2.7	8.2	CSF2	-6.8	10.7
	GSK3B	-2.9	2.6	IRF2BP2	-3.2	7.0	AGT	-6.8	10.1
Muscle	NPC1	2.8	2.5	TEAD1	5.4	21.0	CYP7B1	3.7	6.5
	IRF2BP2	2.7	5.9	RB1	4.7	7.8	miR-3648 (miRNAs	3.7	3.7
	CYP7B1	2.7	7.0	DDX5	4.2	9.5	IGBP1	3.6	6.7
	EPO	2.6	3.8	PPARGC1A	4.2	21.4	DDX5	3.5	7.4
	ZNF106	2.4	3.4	IGBP1	4.0	13.4	FXN	3.5	6.9
	MNT	2.2	2.8	INSR	3.9	19.3	HBA2	3.3	5.8
	GAL3ST1	2.2	3.5	FXN	3.7	18.0	CAB39L	3.3	6.5
	MGP	2.2	2.8	IRF2BP2	3.7	5.6	TEAD1	3.3	10.2
	IL20	-3.6	15.2	DYRK1B	-4.5	22.3	ZHX2	-4.5	12.9
	PTN	-3.6	9.3	TP53	-4.5	7.7	DYRK1B	-4.6	16.1
	MED1	-3.7	4.7	RICTOR	-4.6	12.2	SMARCB1	-4.6	10.4
	SMARCAL1	-3.9	16.2	ADIPOQ	-4.8	18.2	ADIPOQ	-4.6	14.0
	ADIPOQ	-3.9	20.1	CPT1B	-5.1	14.5	CTNNB1	-5.0	3.1
	SMARCB1	-4.7	8.9	HNF1A	-5.2	34.4	RICTOR	-5.1	7.9
	HNF1A	-5.3	33.5	HNF4A	-5.4	37.2	HNF4A	-5.6	33.9
	HNF4A	-5.6	25.0	CLPP	-5.8	34.0	HNF1A	-5.7	22.5
Liver	Irgm1	5.5	10.9				MYCN	7.3	28.3
	SPEN	4.8	7.9				SPEN	6.7	23.4
	MLXIPL	4.7	8.8				Irgm1	5.5	9.7
	CITED2	4.5	11.6				LAPTM5	5.3	8.4
	TTC39A-AS1	4.5	7.8				let-7a-5p (and othe	5.2	10.2
	LAPTM5	4.5	6.2				TRIM38	5.2	13.2
	TREX1	4.4	6.3				LH	5.0	19.6
	IRF2BP2	4.3	17.6				TREX1	4.9	4.2
	IL33	-5.2	15.3				Eldr	-5.9	15.1
	CD44	-5.3	10.1				CD44	-6.0	12.0
	LARP1	-5.6	11.1				TFEB	-6.1	26.0
	TFEB	-5.7	16.9				RICTOR	-6.5	21.8
	TBX3	-5.7	13.1	TFEB	-2.2	2.4	AGT	-6.8	29.4
	CSF2	-6.5	16.3	CPT1B	-2.2	2.1	TBX3	-7.1	11.3
	SLC15A4	-6.5	17.3	CLCF1	-2.2	4.4	interferon alpha	-7.3	10.5
	interferon alpha	-7.2	15.0	EIF6	-2.4	4.3	LARP1	-7.7	36.5
Aorta	NFAT5	3.0	5.8				alpha catenin	4.3	11.5
	INSIG1	2.2	2.7				FKBP10	4.1	14.7
	HFE	2.2	2.5				PSMB11	3.7	6.8
	alpha catenin	2.2	2.6				miR-30c-5p (and c	3.7	5.1
	IRF2BP2	2.2	2.4				MYCN	3.6	4.4
							GRN	3.5	10.7
							miR-29b-3p (and c	3.3	9.5
							COL5A1	3.3	9.9
	CSF2	-2.5	3.5	MAP3K8	-2.2	2.3	CG	-3.8	9.4
	MAPKAPK2	-2.6	6.4	NR1H4	-2.2	5.9	OSM	-3.9	4.9
	PDGF-BB	-2.8	2.1	PPARG	-2.4	2.3	CCR2	-3.9	15.3
	IL1A	-2.9	6.5	SMARCAL1	-2.4	4.8	TWIST1	-4.0	5.6
	HNF1A	-3.1	6.5	ADAM10	-2.4	4.7	TGFB1	-4.4	24.1
	TNF	-3.2	6.1	ADIPOQ	-2.9	5.6	TP53	-4.5	13.5
	IFNG	-3.3	5.3	HNF1A	-3.1	10.6	MAP3K8	-4.6	7.6
	MAP3K8	-3.3	5.5	HNF4A	-3.1	3.3	AGT	-5.7	20.0

Fig. 6. Semaglutide and exercise have synergistic effects on key upstream regulators (URs). UR analysis illustrating the predicted activation state (z-score) of URs, based on expression changes of their target genes. The overlap *P* value indicated significance of the overlap between the known target genes of an UR and the differentially expressed genes measured in the experiment. Red color indicates upregulation and blue color indicates downregulation. The top 8 most significantly upregulated and top 8 most significantly downregulated URs (if applicable) are shown for semaglutide, exercise and the combination of semaglutide with exercise for white adipose tissue (WAT), muscle, liver, and aorta.

miR-29b-3p), consistent with findings from the DEP analysis (Fig. 5D), and deactivating inflammatory regulators (oncostatin M [OSM], C-C motif chemokine receptor 2 [CCR2], TGFB1, MAP3K8).

In summary, UR analysis revealed distinct effects of semaglutide and exercise alone across organs, with the combination treatment showing the largest effects. Furthermore, UR analysis revealed additional regulatory responses, indicating that combining semaglutide with exercise is not merely the sum of the two monotreatments.

DISCUSSION

Besides their effectiveness on glycemic control, GLP-1 receptor agonists like semaglutide have demonstrated significant benefits in treating obesity as well, yet concerns have emerged regarding associated loss of muscle mass during treatment. In this study using HFD-fed Ldlr−/−.Leiden mice, we have demonstrated that exercise partly protects against this semaglutide-induced loss of lean mass, while preserving reductions in fat mass and metabolic benefits. Moreover, while semaglutide alone already had strong beneficial effects, these were further enhanced by adding exercise. The added value of combining semaglutide with exercise was reflected in improved insulin sensitivity, more pronounced reductions in WAT weights, increased weight of gastrocnemius and soleus muscles, enhanced grip strength, and further reductions in hepatic steatosis and a significant reduction in atherosclerotic lesion area with fewer severe atherosclerotic lesions. Detailed histological and transcriptomics analysis revealed both organ-specific and inter-organ effects, providing mechanistic insights that support the added benefit of combining exercise with semaglutide in individuals with metabolic syndrome.

Sarcopenic obesity is associated with a 38% increased risk of developing type 2 diabetes mellitus [13]. Additionally, patients with MASLD and sarcopenia have worse (cardiovascular) outcomes and higher mortality rates [14-16]. Therefore, preservation of lean mass during rapid weight loss is crucial. In this study, semaglutide significantly reduced fat and lean mass. However, when combined with exercise, the reduction in lean mass was attenuated, while fat mass was further reduced. Notably, relative mass of gastrocnemius and soleus increased only in the combination intervention group, whereas the monotreatments separately had no effect. Moreover, combination intervention improved grip strength, indicative of enhanced muscle function as well. In patients with obesity, muscle composition analysis showed significantly lower proportion of type I fibers (slow) and higher proportion of type II fibers (fast) compared to lean individuals, with partial restoration of type I fibers following weight loss [17]. Here, semaglutide alone and with exercise promoted a shift toward type I myofiber composition. These myofibers are associated with better insulin sensitivity due to their higher expression of glucose-handling molecules compared to type II myofibers [18]. Possibly, this shift in myofiber composition contributed to glycemic control as evidenced by the synergistic effect of semaglutide and exercise on lowering insulin levels and thus improving insulin sensitivity. Transcriptomics analysis in muscle further substantiated these additive findings and revealed that only in the combination treatment, pathways concerning glucose metabolism and insulin secretion signaling were affected. In C2C12 myotubes, we found no direct effects of semaglutide on either glucose uptake or myofiber diameter. Furthermore, plasma levels of the muscle-specific marker myostatin were significantly increased only in the combination treatment group. These data support a consistent interpretation that semaglutide may not act directly on muscle fibers but instead improves systemic metabolic conditions that enhance the muscle-adaptive response to exercise. This aligns with growing evidence that GLP-1 receptor agonists exert several acute, weight- and food-intake independent effects that optimize the metabolic environment in which muscle responds to external stimuli. GLP-1 can acutely improve hepatic and muscle insulin sensitivity and reduce endogenous glucose production [19-21], and can enhance insulin action via microvascular recruitment in muscle [22]. It is well known that GLP-1 affects different neural circuits involved in the regulation of energy and metabolism, including the suppression of neuropeptide Y/agouti-related peptide (NPY/AgRP) neurons, thereby immediately affecting metabolism in peripheral tissues [23,24]. For NPY we previously showed that selective sympathetic denervation of the liver could completely block the metabolic effects of NPY on hepatic insulin resistance, while this was not the case for parasympathetic denervation [25]. All together, these acute endocrine, vascular and neural effects offer a concise mechanistic framework explaining how semaglutide primes systemic metabolism and thereby enhances the capacity of exercise to induce metabolic and mitochondrial adaptations. Semaglutide alone already had strong effects on circulating risk factors of metabolic syndrome and adding exercise provided significant additional benefit for

plasma insulin levels only. In the liver, semaglutide improved markers of MASLD, which has been described before in preclinical [26-28] and clinical studies. Here, semaglutide, exercise and to a larger extent their combination all improved steatosis and inflammation in the liver. The latter was further substantiated at the transcriptomics level, where the interventions affected pathways involved in e.g., leukocyte extravasation and acute phase response signaling and URs involved in lipid metabolism. Hepatic fibrosis was not affected by either of the treatments, while in the latest phase 3 trial semaglutide improved steatohepatitis in 63% of the patients, but also reduced hepatic fibrosis in 37% of the patients. This apparent contradiction can be explained by the fact that mice were fed a HFD for 34 weeks in total with treatment during the final 14 weeks. Due to the relatively long half-life of collagen fibers and slow turn-over of matrix remodeling, a 14-week intervention is likely insufficient to produce end-stage histologically detectable changes in fibrosis, whereas *de novo* collagen synthesis is already decreased as we have demonstrated previously for intervention with an fibroblast growth factor 21 (FGF21) mimetic [29]. Furthermore, in our previous study in the same mouse model, we have demonstrated that while semaglutide also in that study did not affect histological fibrosis expressed as percentage of surface area, a more detailed analysis revealed that semaglutide ameliorated the collagen network architecture and significantly decreased the more aggregated collagen fibers in the liver [26]. In the present study, mice treated with semaglutide alone or with exercise, also showed improvements in the circulating marker of fibrosis TIMP1, indicative of reduced extracellular matrix turnover. Taken together with the observation that among the most significantly affected DEPs in the combination treatment group were pathways involved in fibrosis processes, such as collagen biosynthesis, these findings support the hypothesis that a longer treatment duration may ultimately result in detectable antifibrotic effects.

Metabolic syndrome is independently associated with cardiovascular risk and cardiovascular and all-cause mortality [30]. In the vasculature, we have demonstrated that semaglutide reduced heart weight and cardiomyocyte size, which is in line with a previous study in both human subjects and mice [31]. Despite the long exposure to high cholesterol levels, semaglutide monotreatment also tended to reduce atherosclerotic lesion area and combined with exercise atherosclerotic lesion area was significantly reduced. These results were substantiated by the transcriptomics analysis of the aorta that revealed semaglutide indeed affected the atherosclerotic signaling pathway. These observations are in line with the clinical Semaglutide Effects on Cardiovascular Outcomes in People with Overweight or Obesity (SELECT) trial reporting that semaglutide reduced the risk of major adverse cardiovascular events in overweight or obese, but non-diabetic subjects [32].

While the presence of GLP-1 receptors on different tissues is still debated, clearly semaglutide affected directly or indirectly the different tissues examined in our study and demonstrated several beneficial effects. Despite the concomitant loss of lean body mass upon semaglutide, an effect that may become disadvantageous after long-term use of semaglutide, we did not find detrimental effects of semaglutide on muscle function in our study and in fact found several beneficial effects on muscle parameters, in line with the recent "A single-arm, open-label, pilot study of semaglutide for non-alcoholic fatty liver disease" SLIM trial [33]. We observed an increase in type I myofiber proportion and a tendency towards increased myofiber size (as shown by the increase in minimal Feret's diameter) that became significant when combined with exercise. Furthermore, only in the combination group we observed an improved grip strength. Nevertheless, to mitigate any potential long-term effects of semaglutide-induced sarcopenia, especially combined with aging, we strongly recommend accompanying lifestyle advice with sufficient exercise (e.g., resistance training) for semaglutide users. When taking all our data into account, the combination therapy clearly demonstrated the most beneficial effects. The additive value of the combination therapy became evident in the improved insulin levels, improved grip strength, macrovesicular steatosis and atherosclerotic lesion area and was supported by transcriptomics analysis of the different tissues that revealed complementary effects of semaglutide and exercise on several pathways.

Our study demonstrates that combining semaglutide with exercise yields synergistic benefits in the treatment of obesity and metabolic syndrome. While semaglutide alone effectively improves metabolic parameters and reduces fat mass, it also induces a concomitant loss of lean mass and muscle strength. The addition of exercise not only amplifies the beneficial metabolic effects of semaglutide, including enhanced insulin sensitivity and reduced hepatic steatosis and atherosclerosis, but also partially preserves lean mass and improves muscle function. Multi-organ transcriptomic profiling revealed that combination therapy activated distinct molecular pathways not engaged by either intervention alone, underscoring a unique in-

ter-organ crosstalk mechanism. These findings provide compelling evidence that lifestyle interventions can potentiate pharmacological therapies and mitigate their adverse effects, offering a translational strategy to optimize outcomes in patients with obesity and metabolic dysfunction.

SUPPLEMENTARY MATERIALS

Supplementary materials related to this article can be found online at https://doi.org/10.4093/dmj.2025.1060.

CONFLICTS OF INTEREST

No potential conflict of interest relevant to this article was reported.

AUTHOR CONTRIBUTIONS

Conception or design: J.A.I., H.M.G.P., A.M.H.
Acquisition, analysis, or interpretation of data: J.A.I., S.D., J.S., A.L.M., M.P.M.C., J.C.B.C.J., H.M.G.P., A.M.H.
Drafting the work or revising: all authors.
Final approval of the manuscript: all authors.

ORCID

José A. Inia *https://orcid.org/0000-0002-3725-6785*
Aswin L. Menke *https://orcid.org/0000-0002-0724-0897*
Martien P.M. Caspers *https://orcid.org/0000-0002-0248-4008*
Jelle C.B.C. de Jong *https://orcid.org/0000-0002-5154-4900*
J. Wouter Jukema *https://orcid.org/0000-0002-3246-8359*
Hans M.G. Princen *https://orcid.org/0000-0002-7206-1596*
Anita M. van den Hoek *https://orcid.org/0000-0002-7077-8446*

FUNDING

This collaboration project is co-funded by public-private partnership (PPP) Allowance by Health-Holland, Top Sector Life Sciences & Health, to stimulate PPPs.

ACKNOWLEDGMENTS

We thank Anita van Straalen-van Nieuwkoop, Nanda Keijzer, Nicole Worms, Joline Attema, Wim van Duyvenvoorde, Christa de Ruiter, Nikki van Trigt, Lars Verschuren, Angelique Kreikamp and Marijke Voskuilen for their excellent technical assistance. The graphical abstract was created with BioRender.com.

REFERENCES

1. Ahren B, Leguizamo Dimas A, Miossec P, Saubadu S, Aronson R. Efficacy and safety of lixisenatide once-daily morning or evening injections in type 2 diabetes inadequately controlled on metformin (GetGoal-M). Diabetes Care 2013;36:2543-50.
2. Wysham C, Blevins T, Arakaki R, Colon G, Garcia P, Atisso C, et al. Efficacy and safety of dulaglutide added onto pioglitazone and metformin versus exenatide in type 2 diabetes in a randomized controlled trial (AWARD-1). Diabetes Care 2014;37:2159-67.
3. Knudsen LB, Lau J. The discovery and development of liraglutide and semaglutide. Front Endocrinol (Lausanne) 2019;10:155.
4. Gautier JF, Choukem SP, Girard J. Physiology of incretins (GIP and GLP-1) and abnormalities in type 2 diabetes. Diabetes Metab 2008;34 Suppl 2:S65-72.
5. Muller TD, Finan B, Bloom SR, D'Alessio D, Drucker DJ, Flatt PR, et al. Glucagon-like peptide 1 (GLP-1). Mol Metab 2019;30:72-130.
6. Morrison MC, Verschuren L, Salic K, Verheij J, Menke A, Wielinga PY, et al. Obeticholic acid modulates serum metabolites and gene signatures characteristic of human NASH and attenuates inflammation and fibrosis progression in Ldlr-/-.Leiden mice. Hepatol Commun 2018;2:1513-32.
7. van den Hoek AM, Verschuren L, Worms N, van Nieuwkoop A, de Ruiter C, Attema J, et al. A translational mouse model for NASH with advanced fibrosis and atherosclerosis expressing key pathways of human pathology. Cells 2020;9:2014.
8. Morrison MC, Kleemann R, van Koppen A, Hanemaaijer R, Verschuren L. Key inflammatory processes in human NASH are reflected in Ldlr-/-.Leiden mice: a translational gene profiling study. Front Physiol 2018;9:132.
9. Morrison MC, Mulder P, Salic K, Verheij J, Liang W, van Duyvenvoorde W, et al. Intervention with a caspase-1 inhibitor reduces obesity-associated hyperinsulinemia, non-alcoholic steatohepatitis and hepatic fibrosis in LDLR-/-.Leiden mice. Int J Obes (Lond) 2016;40:1416-23.
10. Gart E, Souto Lima E, Schuren F, de Ruiter CG, Attema J, Verschuren L, et al. Diet-independent correlations between bacteria and dysfunction of gut, adipose tissue, and liver: a compre-

hensive microbiota analysis in feces and mucosa of the ileum and colon in obese mice with NAFLD. Int J Mol Sci 2018;20:1.
11. Jacobs SA, Gart E, Vreeken D, Franx BA, Wekking L, Verweij VG, et al. Sex-specific differences in fat storage, development of non-alcoholic fatty liver disease and brain structure in juvenile HFD-induced obese Ldlr-/-.Leiden mice. Nutrients 2019;11:1861.
12. Skurk T, Alberti-Huber C, Herder C, Hauner H. Relationship between adipocyte size and adipokine expression and secretion. J Clin Endocrinol Metab 2007;92:1023-33.
13. Khadra D, Itani L, Tannir H, Kreidieh D, El Masri D, El Ghoch M. Association between sarcopenic obesity and higher risk of type 2 diabetes in adults: a systematic review and meta-analysis. World J Diabetes 2019;10:311-23.
14. Polyzos SA, Vachliotis ID, Mantzoros CS. Sarcopenia, sarcopenic obesity and nonalcoholic fatty liver disease. Metabolism 2023;147:155676.
15. Guo W, Zhao X, Miao M, Liang X, Li X, Qin P, et al. Association between skeletal muscle mass and severity of steatosis and fibrosis in non-alcoholic fatty liver disease. Front Nutr 2022;9:883015.
16. Kouvari M, Polyzos SA, Chrysohoou C, Skoumas J, Pitsavos CS, Panagiotakos DB, et al. Skeletal muscle mass and abdominal obesity are independent predictors of hepatic steatosis and interact to predict ten-year cardiovascular disease incidence: data from the ATTICA cohort study. Clin Nutr 2022;41:1281-9.
17. Tanner CJ, Barakat HA, Dohm GL, Pories WJ, MacDonald KG, Cunningham PR, et al. Muscle fiber type is associated with obesity and weight loss. Am J Physiol Endocrinol Metab 2002;282:E1191-6.
18. Albers PH, Pedersen AJ, Birk JB, Kristensen DE, Vind BF, Baba O, et al. Human muscle fiber type-specific insulin signaling: impact of obesity and type 2 diabetes. Diabetes 2015;64:485-97.
19. Hargrove DM, Nardone NA, Persson LM, Parker JC, Stevenson RW. Glucose-dependent action of glucagon-like peptide-1 (7-37) in vivo during short- or long-term administration. Metabolism 1995;44:1231-7.
20. Wu H, Sui C, Xu H, Xia F, Zhai H, Zhang H, et al. The GLP-1 analogue exenatide improves hepatic and muscle insulin sensitivity in diabetic rats: tracer studies in the basal state and during hyperinsulinemic-euglycemic clamp. J Diabetes Res 2014;2014:524517.
21. Hagve M, Gjessing PF, Hole MJ, Jansen KM, Fuskevag OM, Mollnes TE, et al. Perioperative infusion of glucagon-like peptide-1 prevents insulin resistance after surgical trauma in female pigs. Endocrinology 2019;160:2892-902.
22. Chai W, Zhang X, Barrett EJ, Liu Z. Glucagon-like peptide 1 recruits muscle microvasculature and improves insulin's metabolic action in the presence of insulin resistance. Diabetes 2014;63:2788-99.
23. Heijboer AC, Pijl H, Van den Hoek AM, Havekes LM, Romijn JA, Corssmit EP. Gut-brain axis: regulation of glucose metabolism. J Neuroendocrinol 2006;18:883-94.
24. Kabahizi A, Wallace B, Lieu L, Chau D, Dong Y, Hwang ES, et al. Glucagon-like peptide-1 (GLP-1) signalling in the brain: from neural circuits and metabolism to therapeutics. Br J Pharmacol 2022;179:600-24.
25. van den Hoek AM, van Heijningen C, Schroder-van der Elst JP, Ouwens DM, Havekes LM, Romijn JA, et al. Intracerebroventricular administration of neuropeptide Y induces hepatic insulin resistance via sympathetic innervation. Diabetes 2008;57:2304-10.
26. Inia JA, Stokman G, Morrison MC, Worms N, Verschuren L, Caspers MP, et al. Semaglutide has beneficial effects on non-alcoholic steatohepatitis in Ldlr-/-.Leiden mice. Int J Mol Sci 2023;24:8494.
27. Soto-Catalan M, Opazo-Rios L, Quiceno H, Lazaro I, Moreno JA, Gomez-Guerrero C, et al. Semaglutide improves liver steatosis and de novo lipogenesis markers in obese and type-2-diabetic mice with metabolic-dysfunction-associated steatotic liver disease. Int J Mol Sci 2024;25:2961.
28. Niu S, Chen S, Chen X, Ren Q, Yue L, Pan X, et al. Semaglutide ameliorates metabolism and hepatic outcomes in an NAFLD mouse model. Front Endocrinol (Lausanne) 2022;13:1046130.
29. Inia JA, Attema J, de Ruiter C, Menke AL, Caspers MP, Verschuren L, et al. Therapeutic effects of FGF21 mimetic bFKB1 on MASH and atherosclerosis in Ldlr-/-.Leiden mice. FASEB J 2024;38:e70087.
30. Guembe MJ, Fernandez-Lazaro CI, Sayon-Orea C, Toledo E, Moreno-Iribas C. Risk for cardiovascular disease associated with metabolic syndrome and its components: a 13-year prospective study in the RIVANA cohort. Cardiovasc Diabetol 2020;19:195.
31. Martens MD, Abuetabh Y, Schmidt MA, Zolondek MCP, Silver HL, Levasseur JL, et al. Semaglutide reduces cardiomyocyte size and cardiac mass in lean and obese mice. JACC Basic Transl Sci 2024;9:1429-31.
32. Lincoff AM, Brown-Frandsen K, Colhoun HM, Deanfield J, Emerson SS, Esbjerg S, et al. Semaglutide and cardiovascular

outcomes in obesity without diabetes. N Engl J Med 2023;389: 2221-32.
33. Ditzenberger GL, Lake JE, Kitch DW, Kantor A, Muthupillai R, Moser C, et al. Effects of semaglutide on muscle structure and function in the SLIM LIVER Study. Clin Infect Dis 2025;80: 389-96.

SUPPLEMENTARY METHODS

Experimental design

Males were selected due to their higher susceptibility to obesity and inflammation. Mice (aged 14 to 19 weeks) were group-housed in a temperature-controlled room at 50% to 60% humidity and 12-hour light-dark cycle. Mice received food and water *ad libitum*. Body weight, food intake per cage and clinical signs were monitored regularly. One group ($n=8$) served as healthy control group and received the grain-based chow diet (Ssniff Spezialdiäten, Soest, Germany) and 75 mice received a high-fat diet (HFD) containing 45 kCal% fat from lard, 35 kCal% carbohydrates and 20 kCal% casein (Research Diets, New Brunswick, NJ, USA) to induce metabolic dysfunction-associated steatohepatitis (MASH) and atherosclerosis.

At $t=0$, after a 20-week run-in period on HFD, mice were matched on body weight, age and glucose, cholesterol and triglyceride levels into equal groups ($n=15$). Group sizes were calculated by power analysis (GPower), using a minimal effect size of 30%, two-sided *t*-test with 95% confidence interval, 90% power and α of 0.05. One group served as HFD reference group and was sacrificed at $t=0$ to indicate the histological severity (in particular MASH and atherosclerosis) at the start of the intervention period and determine whether the interventions affected parameters beyond levels at the start of the intervention period or merely blocked further progression. Another group on HFD received daily subcutaneous saline injections (HFD vehicle control) for 14 weeks. The third group on HFD received daily subcutaneous semaglutide injections (100 μL; Ozempic, Novo Nordisk, Bagsværd, Denmark). To acclimatize to the final semaglutide dosage (0.12 mg/kg body weight/day), the dose was escalated over the course of 5 days at a rate of 0.024 (20%), 0.048 (40%), 0.072 (60%), 0.096 (80%) mg/kg body weight/day until the final dose was reached that was maintained for 14 weeks. Doses were adjusted based on weekly individual body weights. For the fourth group of mice on HFD, a running wheel (Mouse Igloo+Fast Trac, Datesand, Bredbury, UK) was added into the cage, to which the mice had unlimited access and which has been shown to increase voluntary movement in these mice [1]. The last group on HFD received both subcutaneous semaglutide injections and a running wheel in the cage. At the study endpoint at $t=14$ weeks (or at $t=0$ for the HFD reference group), mice were sacrificed by gradual fill CO_2 asphyxiation and tissues were collected.

Biochemical analyses

Liver tissue, hearts with aortic roots, ascending aortas, perigonadal white adipose tissue (pgWAT) and subcutaneous white adipose tissue and brown adipose tissue were collected. Left gastrocnemius and soleus muscles were isolated jointly and right gastrocnemius and quadriceps were isolated separately. Tissues were snap-frozen in liquid nitrogen for biochemical/transcriptome analyses or formalin-fixed and paraffin-embedded (FFPE) for histological analyses.

Lean and fat mass were determined at several timepoints using an NMR EchoMRI whole-body composition analyzer (EchoMRI 2-in-1, Echo Medical Systems LTD, Houston, TX, USA). Two paw grip strength was measured using a grip force meter (TSE Systems GmbH, Bad Homburg, Germany). To this end, mice were placed on a grid attached to a force gauge and steadily pulled by the tail. Per mouse, five trials were performed with 1 minute resting intervals, the highest and lowest values for maximum strength produced before releasing the grid were excluded and averages of the remaining three trials were taken.

Blood was drawn at several timepoints from the tail vein into ethylenediaminetetraacetic acid-coated tubes (Sarstedt, Nümbrecht, Germany) after a 5-hour fasting period. At the time of blood sampling, blood glucose concentrations were determined using a hand analyzer and glucose strips (FreeStyle Lite, Chicago, IL, USA). Plasma insulin concentrations were measured by enzyme-linked immunosorbent assay (ELISA) (#90080; Crystal Chem, Elk Grove Village, IL, USA). Plasma cholesterol and triglyceride levels were measured using enzymatic colorimetric assays (Roche Diagnostics, Almere, the Netherlands). Plasma alanine transaminase concentrations were determined by SimpleStep ELISA (Abcam, Cambridge, UK). Plasma TIMP1 (DY980; R&D Systems, Abingdon, UK) and plasma myostatin (DY788-05; R&D Systems) were all measured by ELISA. Plasma interleukin 6 and brain-derived neurotrophic factor were measured using a multiplex immunoassay panel (U-PLEX Assay Platform, Mesoscle Discovery [MSD], Rockville, MD, USA) in accordance with the manufacturer's protocol on a MEDO QuickPlex SQ 120 reader (MSD).

Histological assessment of adipose tissue

A pgWAT (FFPE) was cross-sectioned (5 μm) and stained with hematoxylin-phloxine-saffron (HPS). Adipocyte size was analyzed in ImageJ version 1.53 (National Institutes of Health, Bethesda, MD, USA) using the Adiposoft plugin [2] in three randomly selected non-overlapping fields (view size 2.4 mm^2)

as described previously in detail [3-5]. Inflammation was analyzed in the same fields by counting the number of crown-like structures and expressed as number per 1,000 adipocytes [3-5].

Histological and biochemical assessment of muscle tissue

Jointly isolated tissue of the soleus and gastrocnemius (FFPE) was cross-sectioned (5 μm) at the thickest part. Epitope retrieval was performed by incubating slides in 10 mM sodium citrate (pH 6.0) at 95°C for 25 minutes, followed by blocking of endogenous peroxidase activity using 0.3% hydrogen peroxide (v/v) for 10 minutes. Slides were then blocked in 5% normal goat serum in Tris-buffered saline (TBS) for 30 minutes, followed by overnight incubation with a primary antibody mixture containing anti-myosin heavy chain 7 (MYH7; for slow myofibers) (SAB4200670-1:200; Sigma-Aldrich, Burlington, MA, USA) and laminin (for basal lamina) (NB300-144-1:100; Novus Biologicals, Centennial, CO, USA) in 1% normal goat serum at 4°C. Subsequently, slides were incubated with a secondary antibody mixture containing goat anti-rabbit horseradish peroxidase (HRP) (Ab6721-1:400, Abcam) and goat anti-mouse alkaline phosphatase (Ab7069-1:400, Abcam) for 1 hour at room temperature. Slides were developed using an HRP substrate kit (SK-4700, Vector Laboratories, Burlingame, CA, USA) and alkaline phosphatase substrate kit (SK-5100, Vector Laboratories) in accordance with the manufacturer's protocols. Slides were scanned with the Pannoramic 500 scanner at 20× magnification. In the soleus muscle, MYH7-positive type I (slow) myofibers were counted and expressed as percentage of total myofibers. In the gastrocnemius muscle, minimal Feret's diameter, reported to be least sensitive for sectioning angle of the muscle [6], was measured using ImageJ for 15 muscle fibers in three randomly selected areas (view size 4.5 mm^2), yielding 45 measurements per mouse. In the gastrocnemius muscle, fiber density was measured manually in three randomly selected areas (view size 2.6 mm^2). Density of muscle fibers was calculated as the total number of muscle fibers relative to the total area of muscle fibers analyzed. Intramuscular triglycerides, were determined in snap-frozen homogenized gastrocnemius samples, from which lipids had been extracted as described previously [7]. Lipids were separated by high performance thin layer chromatography, stained with a color reagent (5 g $MnCl_2{\cdot}4H_2O$, 32 mL 95%–97% H_2SO_4 added to 960 mL of CH_3OH:H_2O 1:1 v/v) and quantified using Image Lab software version 5.2.1 (Bio-Rad Laboratories B.V., Veenendaal, the Netherlands).

***In vitro* muscle analysis**

Murine C2C12 myoblasts (American Type Culture Collection [ATCC], CRL-1772) were cultured in high-glucose Dulbecco's Modified Eagle Medium (DMEM) supplemented with 10% fetal calf serum, 1% penicillin-streptomycin, and 1% GlutaMAX (Sigma-Aldrich) at 37°C and 5% CO_2. Cells were seeded at 12,500 cells/well in 24-well plates and differentiated at approximately 90% confluency (day 0) using DMEM containing 2% horse serum, 1% penicillin-streptomycin, 1% glutamax, and 1% sodium pyruvate (Sigma-Aldrich). Differentiation medium was refreshed every other day. On day 6–7, myotubes were used for morphological or functional assays. To assess the effects of semaglutide on differentiation, cells were treated with 1, 10, or 100 nM semaglutide from day 0. Prostaglandin D_2 (10 μM, Sigma-Aldrich) served as a negative control [8]. On day 6, cells were fixed in methanol and stained with Jenner-Giemsa [9]. Myofiber morphology was evaluated by microscopy, and ImageJ was used to quantify minimal Feret's diameter and fusion index (percentage of nuclei within myotubes; approximately 490±95 nuclei/well) [8]. For glucose uptake, 6-day differentiated myotubes were serum-deprived and treated with semaglutide (1–100 nM) for 16 hours. After phosphate-buffered saline and buffer washes, glucose uptake was measured using a bioluminescent 2-deoxyglucose assay (Promega, Madison, WI, USA; J1341). Insulin (5 nM, Sigma-Aldrich) was used as a positive control. Each condition was assessed in replicate wells across multiple experiments (n=5–6 measurements, n=3 for insulin positive control, and n=4 for prostaglandin D_2 negative control).

Histological assessment of the liver

Tissue of the left liver lobe (FFPE) was cross-sectioned (3 μm) and stained with hematoxylin and eosin (H&E) or Sirius Red (SR). Presence of metabolic dysfunction-associated steatotic liver disease (MASLD) was evaluated by a board-certified pathologist in two liver slides per mouse and by using an adapted grading system of human MASLD [10,11]. Macrovesicular and microvesicular steatosis were determined in H&E-stained slides at 40× magnification and expressed as percentage of the total analyzed surface area. Inflammation was scored in H&E-stained slides by counting the number of aggregated inflammatory cells per field at 100× magnification. Five random, non-overlapping fields (view size 4.2 mm^2) were scored and data were expressed as average score per mm^2. Fibrosis was scored in SR-stained slides with computerized analysis and

positive staining was expressed as percentage of total analyzed liver surface. Fibrosis stage was scored in the same slides by the board-certified pathologist consistent with the adapted scoring protocol by Tiniakos et al. [12]. Accordingly, fibrosis was scored as absence of fibrosis (F0), fibrosis within perisinusoidal/perivenular or periportal area (F1), fibrosis within both perisinusoidal and periportal areas (F2), bridging fibrosis (F3) or cirrhosis (F4).

Histological assessment of vasculature

Heart tissue (FFPE) was cross-sectioned (5 μm) at 50 μm intervals perpendicular to aorta axis. Sections were stained with HPS and scanned with the Pannoramic 500 scanner (3DHISTECH Ltd., Budapest, Hungary). Atherosclerosis was evaluated in four sections per mouse at 50 μm intervals and total lesion area per cross-section was determined in SlideViewer version 2.8 (3DHISTECH Ltd.). Lesion severity was scored into five categories in line with the American Heart Association classification. Accordingly, lesions are classified as undiseased (0), early fatty streak (type I), regular fatty streak (type II), mild plaque (type III), moderate plaque (type IV), or severe plaque (type V) [13,14].

Additional heart tissue (FFPE) was cross-sectioned (5 μm) and epitope retrieval was performed by incubating slides in 10 mM sodium citrate (pH 6.0) at 95°C for 25 minutes, followed by blocking of endogenous peroxidase activity using 0.3% hydrogen peroxide (v/v) for 10 minutes. Slides were then blocked in 5% normal goat serum in TBS for 30 minutes, followed by overnight incubation with laminin (for basal lamina) (NB300-144-1:100, Novus Biologicals) in 1% normal goat serum at 4°C. Subsequently, slides were incubated with a goat anti-rabbit HRP secondary antibody (Ab6721-1:400; Abcam) for 1 hour at room temperature. Slides were developed using an HRP substrate kit (SK-4700, Vector Laboratories) in accordance with the manufacturer's protocols. Slides were scanned with the Pannoramic 500 scanner at 20× magnification. Cardiomyocyte size was determined in the left ventricular wall in one randomly selected field per mouse (view size: 0.06 mm^2). Cardiomyocyte size was quantified using customized macros in ImageJ, yielding measurement of approximately 100 cells per mouse.

Transcriptomics

For transcriptomics analysis, snap-frozen tissue of the right liver lobe, right quadriceps femoris, pgWAT and ascending aorta were used. RNA was extracted using the RNA-Stat60 total RNA isolation kit (Amsbio, Cambridge, UK) for liver, muscle and aorta and using the Ambion RNAqueous total RNA isolation kit (ThermoFisher Scientific, Waltman, MA, USA) for white adipose tissue (WAT).

Total RNA was processed into tagged random sequence libraries (NEBNext Ultra II Directional RNA Library Prep Kit for Illumina, NEB #E7760S/L, Biolabs, Cambridge, MA, USA) and a quality check for proper size distribution was performed (300–500 bp peak, Fragment Analyzer). Mixed (multiplex) sample libraries were sequenced at GenomeScan BV (Leiden, the Netherlands) on an Illumina NovaSeq6000 sequencer with a pair-read 150-cycle sequencing protocol, yielding in approximately 20–40 million read counts per sample. A concentration of 1.1 nM DNA was used yielding paired-end reads (2×150 basepairs) and NovaSeq control software (NCS version 1.7) was used. Image analysis, base calling, and quality check was performed with the Illumina data analysis pipeline RTA3.4.4 and Bcl2fastq v2.20. Trimmed Fastq files were merged (in case of paired-end reads) and aligned to the reference genome (Mus_musculus.GRCm38.gencode.vM19) using the STAR 2.5 algorithm with default settings (https://github.com/alexdobin/STAR). Based on the mapped read locations and the gene annotation, Htseq-count 0.6.1p1 was used to obtain the read mapping frequency per gene per sample (counts), that subsequently served as input for the differentially expressed genes analysis using the DESeq2-method.32. Due to technical issues (% reads mapped to too many loci) with in particular WAT and aorta tissue some samples had to be excluded from further analysis, ultimately resulting in analysis of $n \geq 14$ (and $n=8$ for chow) for muscle and liver, but $n=7$ chow, $n=10$ HFD control, $n=7$ semaglutide, $n=10$ exercise and $n=8$ combination mice for WAT and $n=4$ chow, $n=7$ HFD control, $n=8$ semaglutide, $n=9$ exercise and $n=7$ combination mice for aorta. These were used as input for pathway analysis through Ingenuity Pathway Analysis (IPA; Ingenuity Systems Inc., Redwood City, CA, USA, accessed May 2025). IPA uses gene expression data of known downstream target genes to predict the activation state or deactivation state of upstream regulators (e.g., transcription factors, signaling proteins, and metabolites). Area-proportional Venn diagrams were prepared using the web application of Hulsen et al. [15]. The datasets obtained in this study are accessible at the National Center for Biotechnology Information (NCBI) Gene Expression Omnibus (GEO-ID: GSE304862).

SUPPLEMENTARY REFERENCES

1. van den Hoek AM, de Jong JCBC, Worms N, van Nieuwkoop A, Voskuilen M, Menke AL, et al. Diet and exercise reduce preexisting NASH and fibrosis and have additional beneficial effects on the vasculature, adipose tissue and skeletal muscle via organ-crosstalk. Metabolism 2021;124:154873.
2. Galarraga M, Campion J, Munoz-Barrutia A, Boque N, Moreno H, Martinez JA, et al. Adiposoft: automated software for the analysis of white adipose tissue cellularity in histological sections. J Lipid Res 2012;53:2791-6.
3. Morrison MC, Verschuren L, Salic K, Verheij J, Menke A, Wielinga PY, et al. Obeticholic acid modulates serum metabolites and gene signatures characteristic of human NASH and attenuates inflammation and fibrosis progression in Ldlr-/-.Leiden mice. Hepatol Commun 2018;2:1513-32.
4. Jacobs SAH, Gart E, Vreeken D, Franx BAA, Wekking L, Verweij VGM, et al. Sex-specific differences in fat storage, development of non-alcoholic fatty liver disease and brain structure in juvenile HFD-induced obese Ldlr-/-.Leiden mice. Nutrients 2019;11:1861.
5. Tengeler AC, Gart E, Wiesmann M, Arnoldussen IAC, van Duyvenvoorde W, Hoogstad M, et al. Propionic acid and not caproic acid, attenuates nonalcoholic steatohepatitis and improves (cerebro) vascular functions in obese Ldlr-/-.Leiden mice. FASEB J 2020;34:9575-93.
6. Briguet A, Courdier-Fruh I, Foster M, Meier T, Magyar JP. Histological parameters for the quantitative assessment of muscular dystrophy in the mdx-mouse. Neuromuscul Disord 2004;14:675-82.
7. Post SM, de Crom R, van Haperen R, van Tol A, Princen HM. Increased fecal bile acid excretion in transgenic mice with elevated expression of human phospholipid transfer protein. Arterioscler Thromb Vasc Biol 2003;23:892-7.
8. Velica P, Khanim FL, Bunce CM. Prostaglandin D2 inhibits C2C12 myogenesis. Mol Cell Endocrinol 2010;319:71-8.
9. Velica P, Bunce CM. A quick, simple and unbiased method to quantify C2C12 myogenic differentiation. Muscle Nerve 2011;44:366-70.
10. Kleiner DE, Brunt EM, Van Natta M, Behling C, Contos MJ, Cummings OW, et al. Design and validation of a histological scoring system for nonalcoholic fatty liver disease. Hepatology 2005;41:1313-21.
11. Liang W, Menke AL, Driessen A, Koek GH, Lindeman JH, Stoop R, et al. Establishment of a general NAFLD scoring system for rodent models and comparison to human liver pathology. PLoS One 2014;9:e115922.
12. Tiniakos DG, Vos MB, Brunt EM. Nonalcoholic fatty liver disease: pathology and pathogenesis. Annu Rev Pathol 2010;5:145-71.
13. Pouwer MG, Pieterman EJ, Worms N, Keijzer N, Jukema JW, Gromada J, et al. Alirocumab, evinacumab, and atorvastatin triple therapy regresses plaque lesions and improves lesion composition in mice. J Lipid Res 2020;61:365-75.
14. Kuhnast S, van der Hoorn JW, van den Hoek AM, Havekes LM, Liau G, Jukema JW, et al. Aliskiren inhibits atherosclerosis development and improves plaque stability in APOE*3Leiden. CETP transgenic mice with or without treatment with atorvastatin. J Hypertens 2012;30:107-16.
15. Hulsen T, de Vlieg J, Alkema W. BioVenn: a web application for the comparison and visualization of biological lists using area-proportional Venn diagrams. BMC Genomics 2008;9:488.

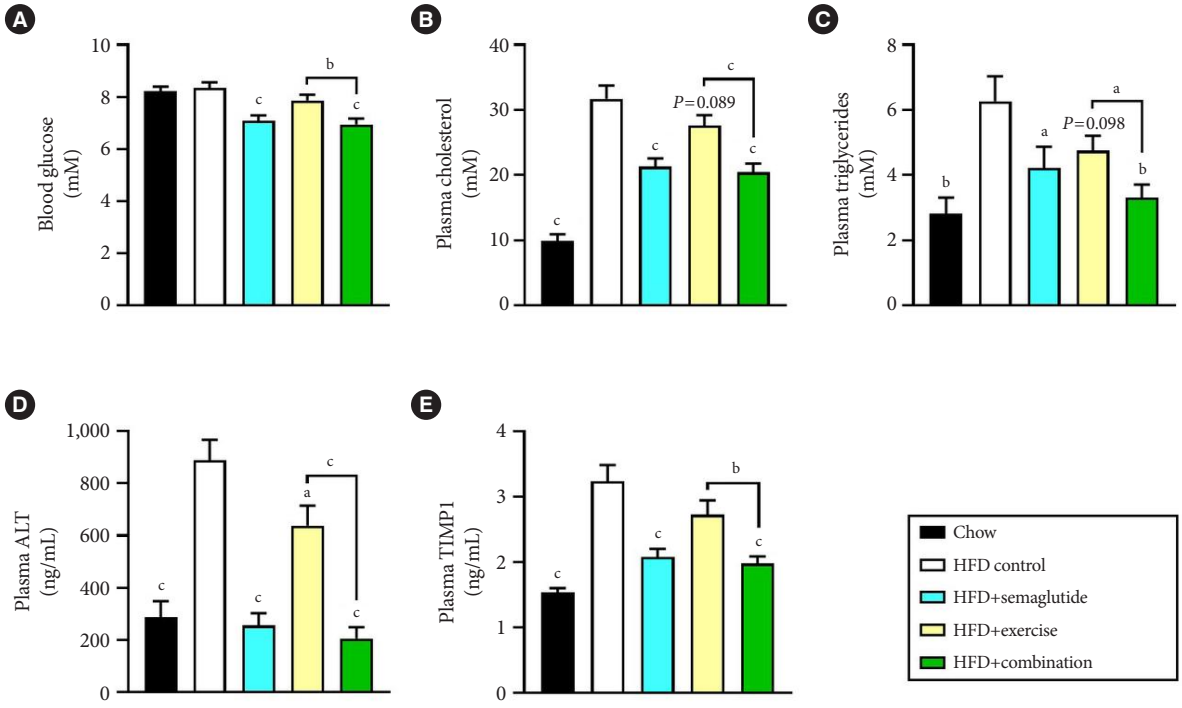

Supplementary Fig. 1. Semaglutide alone and with exercise improve metabolic parameters in obese Ldlr−/−.Leiden mice. Blood glucose (A), plasma cholesterol (B), plasma triglycerides (C) plasma alanine transaminase (ALT) (D) and plasma tissue inhibitor of metalloproteinases 1 (TIMP1) (E). Values are presented as mean±standard error of the mean for $n=14–15$ mice. [a]$P<0.05$, [b]$P<0.01$, [c]$P<0.001$ vs. high-fat diet (HFD) control.

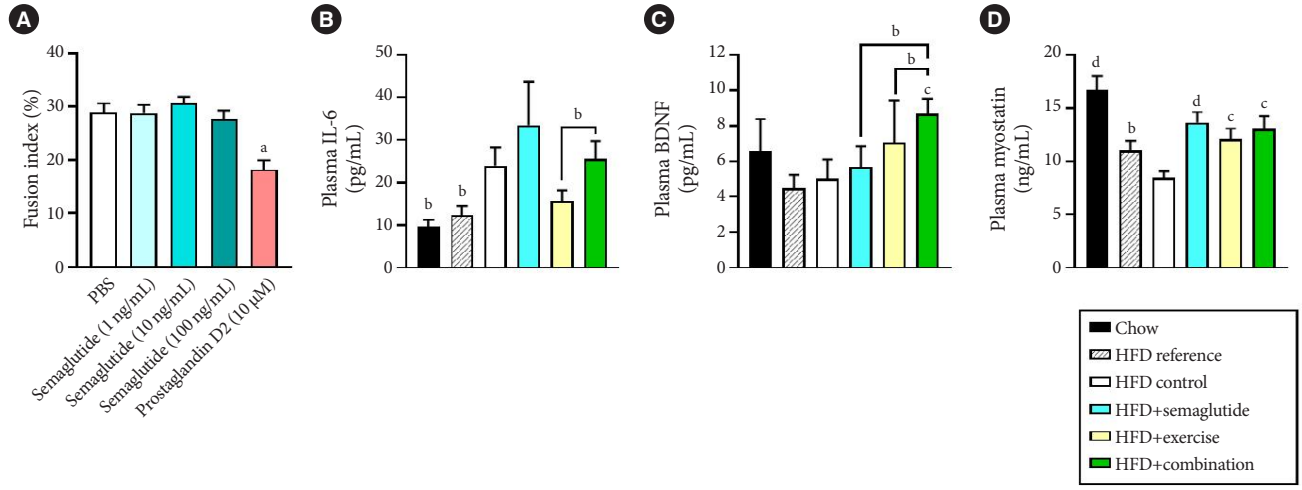

Supplementary Fig. 2. *In vitro* experiment in C2C12 myotubes illustrating fusion index. Values are presented as mean ± standard error of the mean for $n=6$ wells (A). Plasma interleukin 6 (IL-6) (B), brain-derived neurotrophic factor (BDNF) (C), and myostatin (D). Values are presented as mean ± standard error of the mean for $n=14$–15 mice. [a]$P<0.05$ vs. phosphate-buffered saline (PBS); [b]$P<0.05$, [c]$P<0.01$, [d]$P<0.001$ vs. high-fat diet (HFD) control.